

Deeply Virtual Compton Scattering off ^4He

M. Hattawy

(On behalf of the CLAS collaboration)

New Directions in Nuclear Deep Inelastic Scattering

ETC*: 08 – 12 June 2015, Trento, Italy

Outline

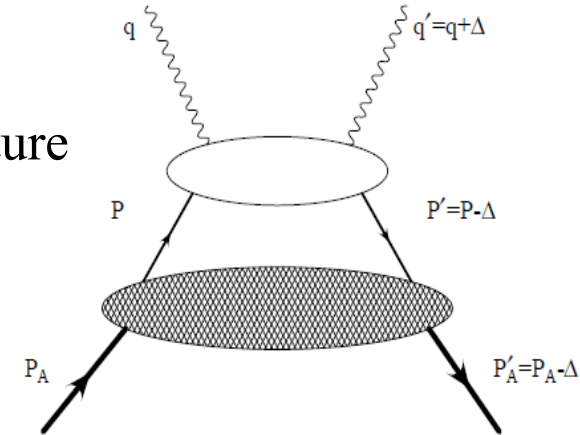
- **Physics motivations.**
- **CLAS-E08-24 experiment @ JLab.**
- **DVCS analysis techniques.**
- **Results, conclusions and perspectives.**

DVCS off nuclei

Two DVCS channels are accessible with nuclear targets:

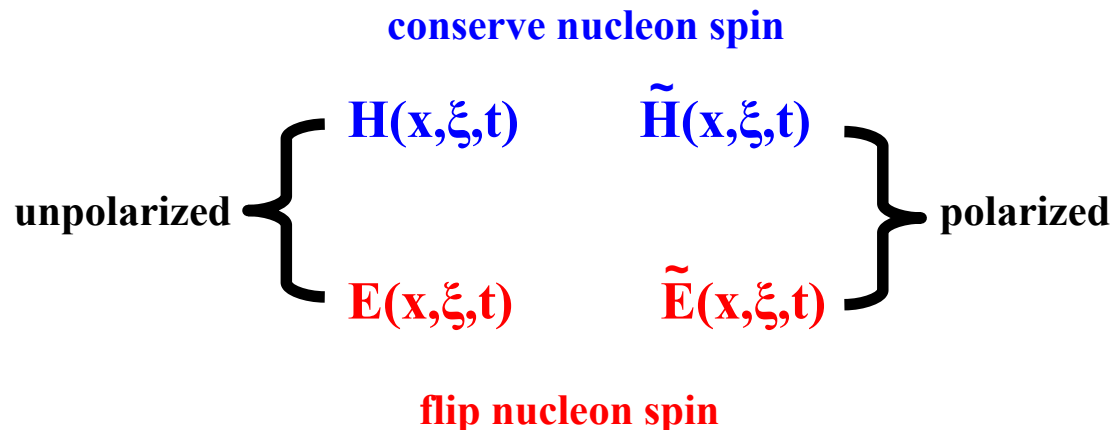
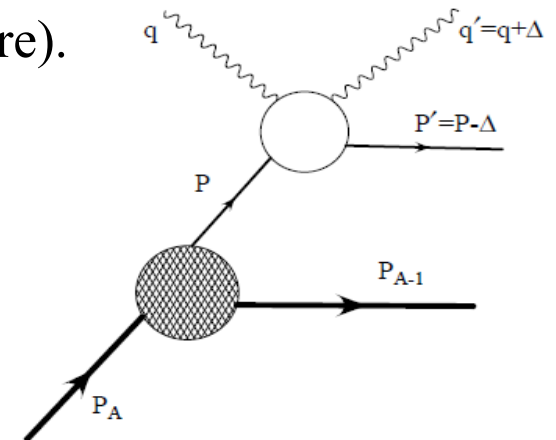
◇ Coherent DVCS: $e^- A \rightarrow e^- A \gamma$

- Study the partonic structure of the nucleus.
- **One chiral-even GPD** (H_A) is needed to parametrize the structure of the **spinless nuclei** (^4He , ^{12}C , ^{16}O , ...).



◇ InCoherent DVCS: $e^- A \rightarrow e^- NX \gamma$

- The nucleus breaks and the DVCS takes place on a nucleon.
- Study the partonic structure of the bound nucleons (**4 chiral-even GPDs** are needed to parametrize their structure).



Nuclear spin-zero DVCS observables

The GPD \mathcal{H}_A parametrizes the structure of the **spinless nuclei** ($^4\text{He}, ^{12}\text{C} \dots$)

$$\mathcal{H}_A(\xi, t) = \text{Re}(\mathcal{H}_A(\xi, t)) - i\pi \text{Im}(\mathcal{H}_A(\xi, t))$$

$$\text{Im}(\mathcal{H}_A(\xi, t)) = H_A(\xi, \xi, t) - H_A(-\xi, \xi, t)$$

$$\text{Re}(\mathcal{H}_A(\xi, t)) = \mathcal{P} \int_0^1 dx [H_A(x, \xi, t) - H_A(-x, \xi, t)] [C^+(x, \xi)]$$

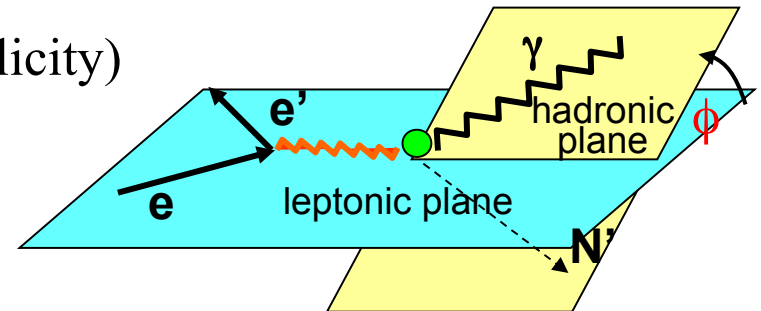
Quark propagator

$$C^+(x, \xi) = \frac{1}{x - \xi} + \frac{1}{x + \xi}$$

◇ $A_{LU}(\phi)$ is mostly sensitive to **Im(\mathcal{H}_A)**: (+/- beam helicity)

$$A_{LU}(\phi) = \frac{1}{P_B} \frac{N^+ - N^-}{N^+ + N^-}$$

$$= \frac{\alpha_0(\phi) * \text{Im}(\mathcal{H}_A)}{\alpha_1(\phi) + \alpha_2(\phi) \text{Re}(\mathcal{H}_A) + \alpha_3(\phi) (\text{Im}(\mathcal{H}_A)^2 + \text{Re}(\mathcal{H}_A)^2)}$$



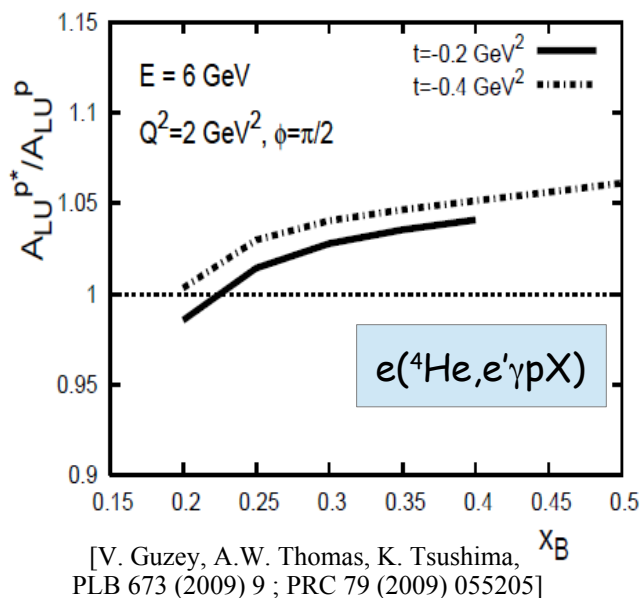
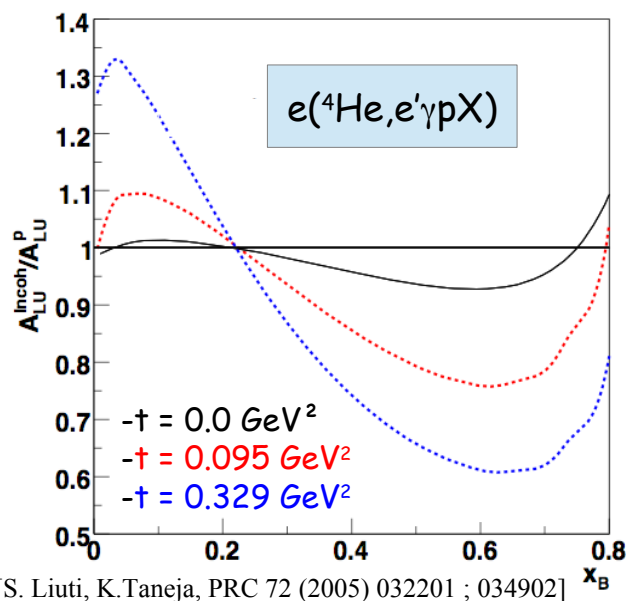
◇ $A_C(\phi)$ is mostly sensitive to **Re(\mathcal{H}_A)**:

(unpolarized leptons of opposite charges on unpolarized target)

$$A_C(\phi) = \frac{N^+ - N^-}{N^+ + N^-} \propto \frac{-\cos(\phi) * \text{Re}(\mathcal{H}_A)}{F_A^{e.m.}(t)}$$

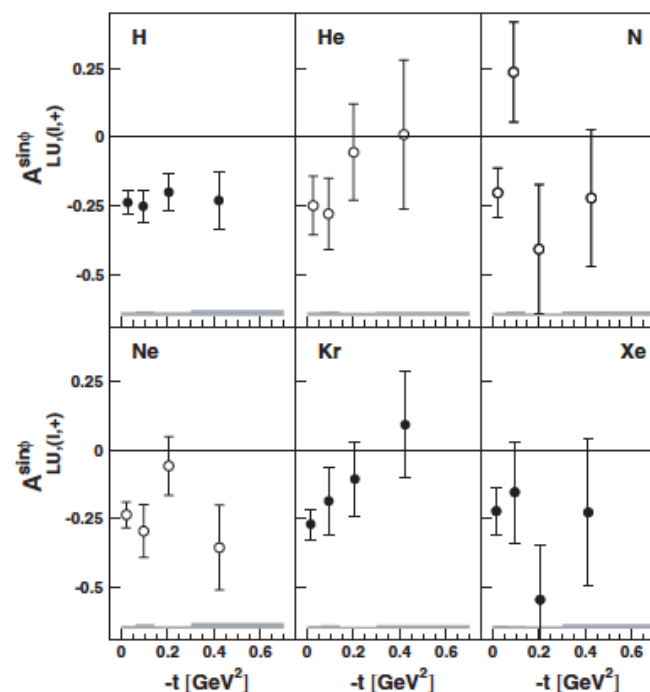
EMC: Helium-4 (2/2)

- Theoretical predictions of the EMC in ^4He , based on GPDs formalism.



- Inclusive measurements of nuclear DVCS @ HERMES

$$A_{LU}^{\text{sin}} = \frac{1}{\pi} \int_0^{2\pi} d\phi \sin \phi A_{LU}(\phi)$$



[A. Airapetian, et al., Phys. Rev. C 81, 035202 (2010)]

In CLAS- E08-024, we measure EXCLUSIVE coherent and incoherent DVCS channels off ^4He

CLAS - E08-024 experimental setup

$$e^- \text{ } ^4\text{He} \rightarrow e^- \text{ } (^4\text{He}/pX) \gamma$$

6 GeV,
L. polarized

Beam polarization (P_B) = 83%

- CLAS:

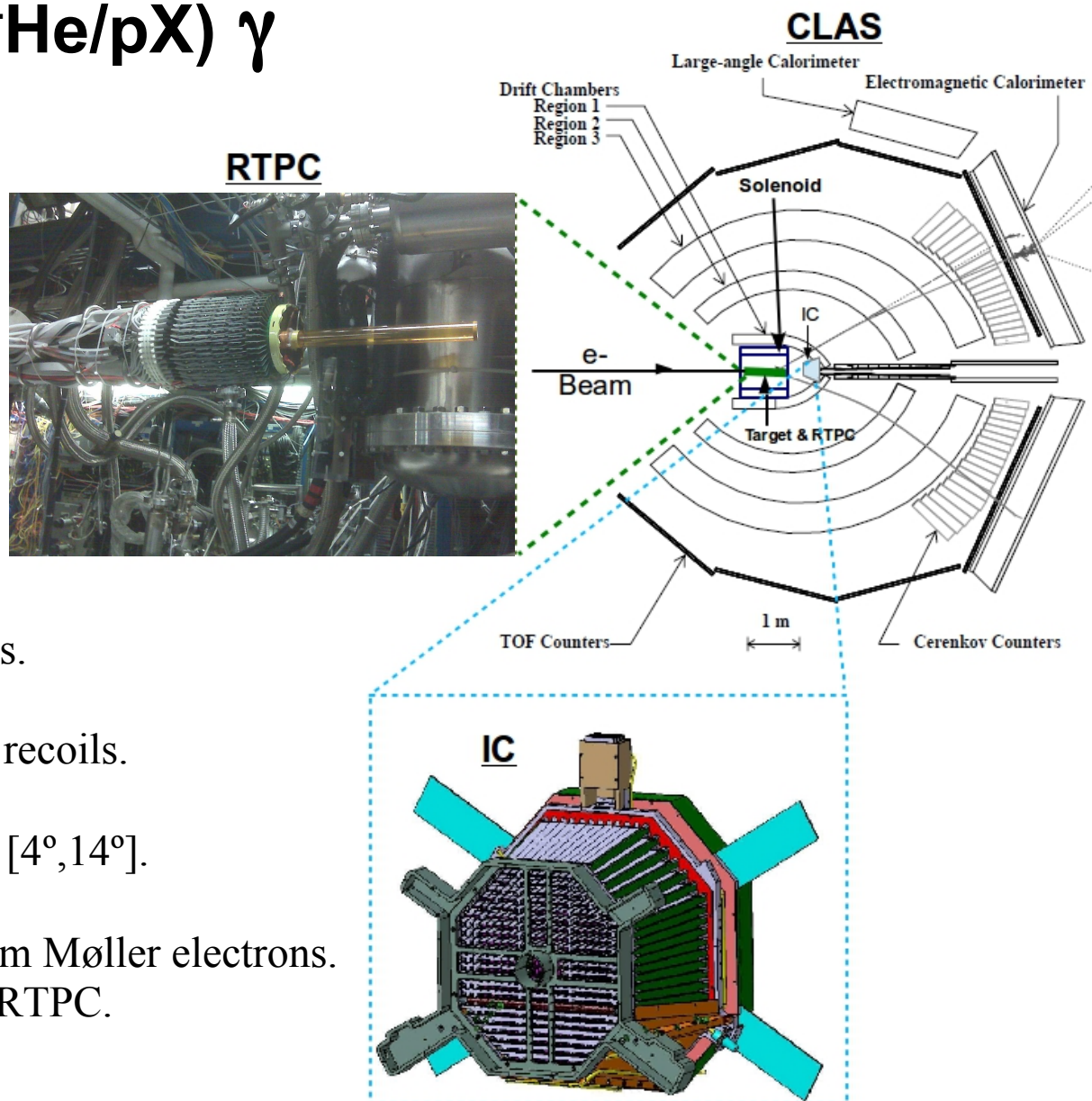
- Superconducting **Torus** magnet.
- 6 independent sectors:
 - **DCs** track charged particles.
 - **CCs** separate e^-/π^- .
 - **ECs** detect γ , e^- and n [$8^\circ, 45^\circ$].
 - **TOF Counters** identify hadrons.

- **RTPC:** Detects low energy nuclear recoils.

- **IC:** Improves γ detection acceptance [$4^\circ, 14^\circ$].

- **Solenoid:** - Shields the detectors from Møller electrons.
- Enables tracking in the RTPC.

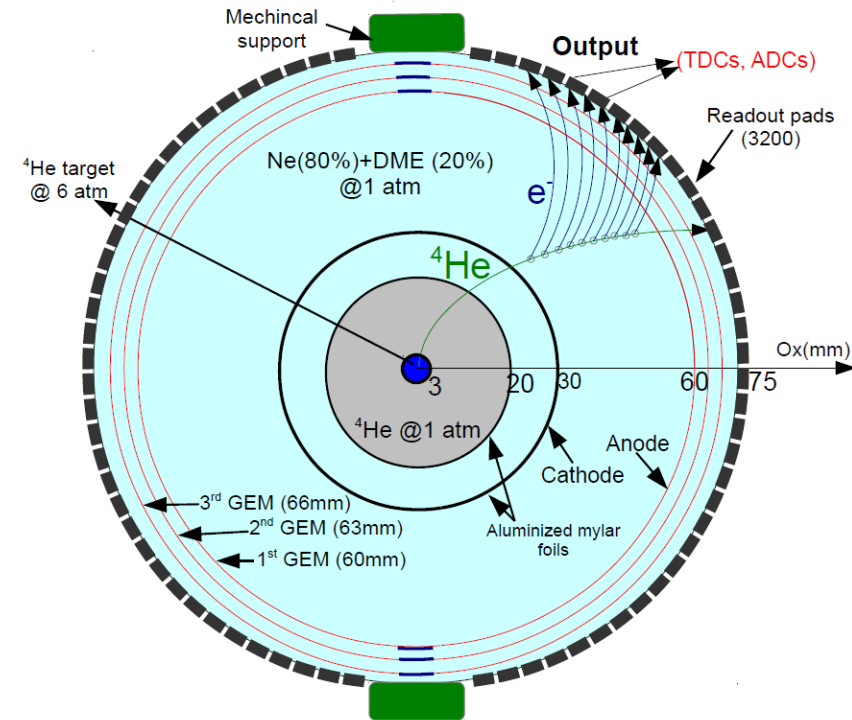
- **Target:** ^4He gas @ 6 atm, 293 K



RTPC

- Design:

- ◆ 80% azimuthal coverage
- ◆ 200 mm long , 15 mm Ø
- ◆ 2 gas gaps to reduce the noise
- ◆ 27 μm cathode foil @ 4.3 kV
- ◆ 30 mm drift region, Ne-DME mixture (80%-20%), @ 1 atm, uniform $|\vec{E}| = 500 \text{ V/cm}$, $|\vec{B}| = 4 \text{ T}$
- ◆ 3 GEMs layers, gain of 1000/layer
- ◆ 3200 readout elements



- Work principle:

Charged particle ionizes the gas atoms

→ Under \vec{E} effect, released electrons follow their **drift paths** at a certain **drift speed**

→ Amplifications via the 3 GEM layers

→ Readout board, record electrons' charges (**ADCs units**) in time bins (**TDCs units**).

- Offline reconstruction:

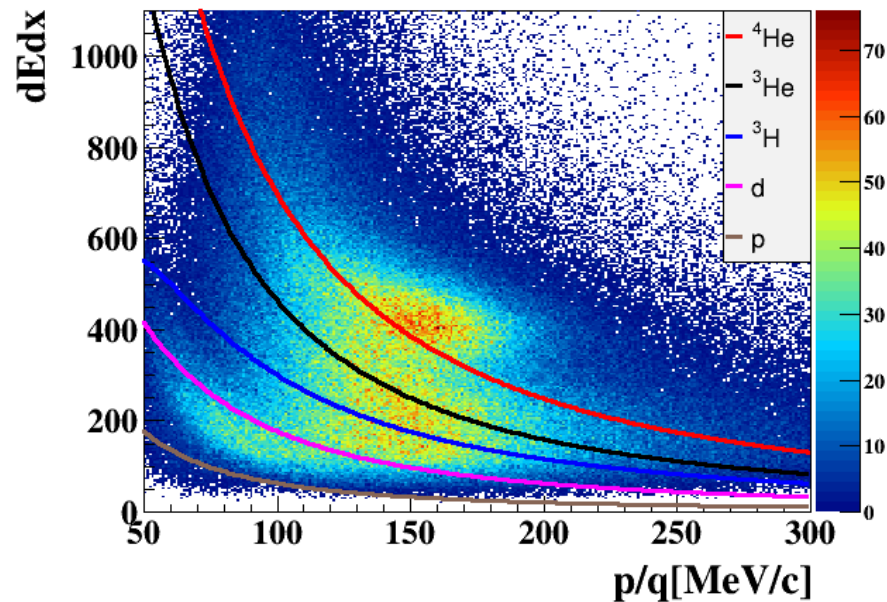
$$\text{ADCs} \xrightarrow{\text{Pads' gains } (G_i)} \left\langle \frac{dE}{dX} \right\rangle = \frac{\sum_i \frac{ADC_i}{G_i}}{v t l}$$

$$\text{TDCs} \xrightarrow{\text{Drift speed and paths}} \text{Reconstructing chains of hits} \xrightarrow{\text{Known } \vec{B}} p/q \quad \left. \vphantom{\text{Reconstructing chains of hits}} \right\} \text{PID}$$

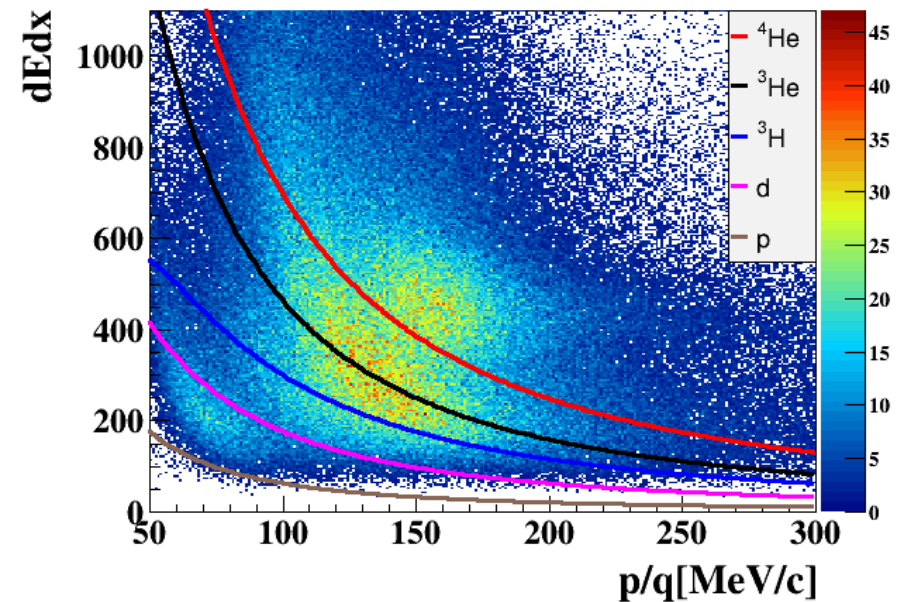
RTPC: gains calibration (2/2)

► $dEdx_{\text{exp}}$ vs. p/q for all the tracks in the RTPC:

Left side



Right side

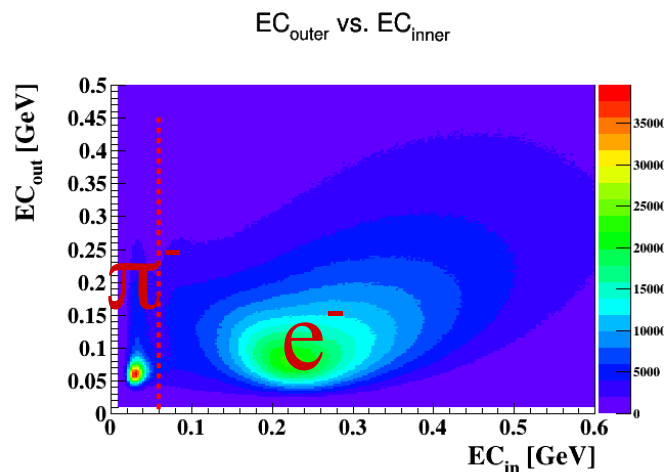


We see separation between the different recoils

PID @ 6 GeV beam energy

- In CLAS, the e^- triggers the DAQ system to record other particles in coincidence.
- We request a set of criteria to identify the electrons and to ensure their detection quality:

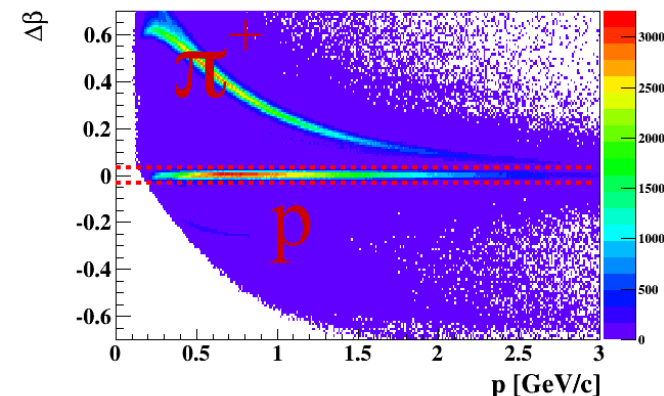
- **Vertex** cut.
- **Fiducial** cuts.
- **EC** energy cut
- **Nphe** in the CCs.



- Proton selection:

- **Vertex** cut.
- **Fiducial** cuts.
- Vertex correspondence.
- Velocity cut ($\Delta\beta$):

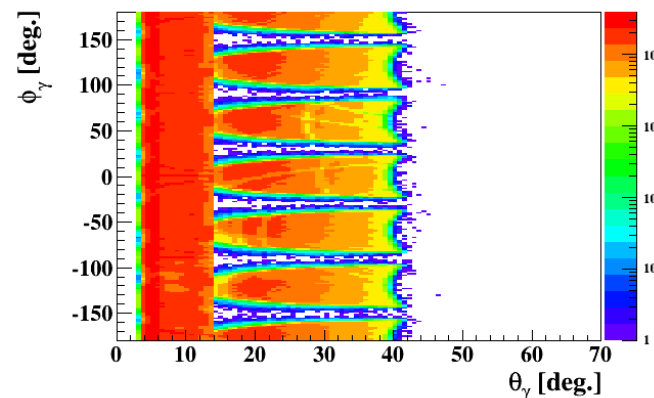
$$\Delta\beta = \beta_{SC} - \beta_{DC} = \frac{l_{track}}{t_{TOF}} - \frac{p}{\sqrt{p^2 + m_p^2}}$$



- Photon selection ($E_\gamma > 300$ MeV):

IC photons $\theta[4^\circ, 14^\circ]$: - IC **fiducial** cut.
 - **Møller electrons** cut.

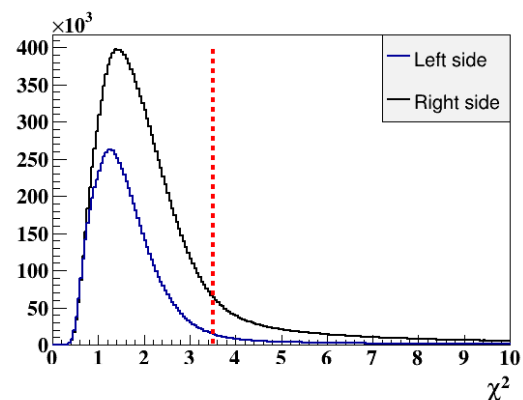
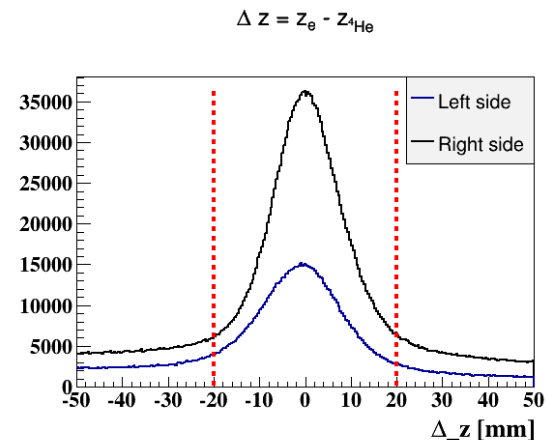
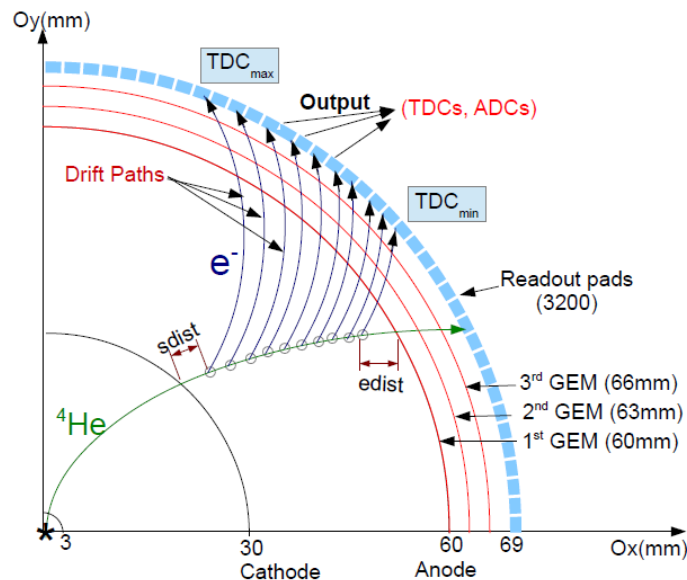
EC photons $\theta[15^\circ, 45^\circ]$: - **EC** fiducial cut.
 - **Velocity** cut.



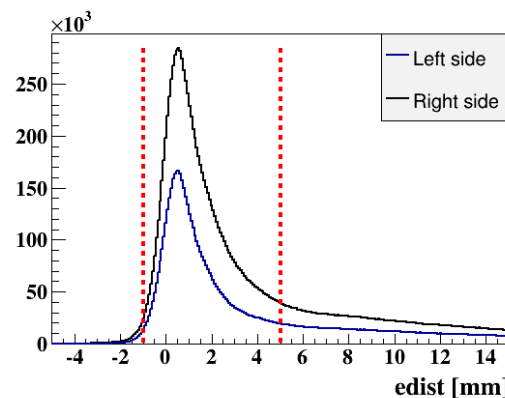
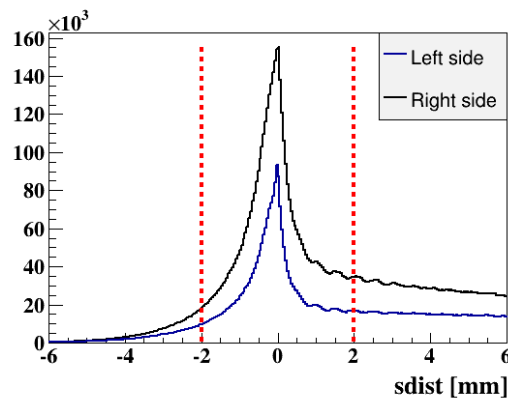
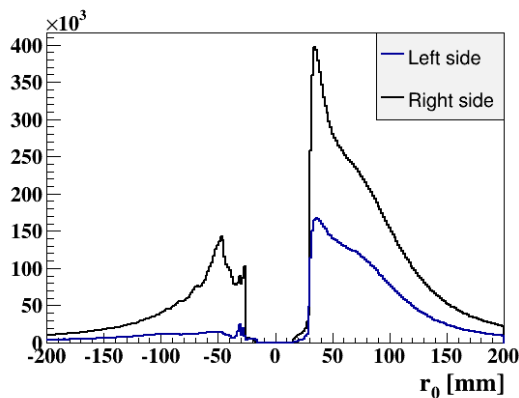
PID @ 6 GeV beam energy: Helium-4

► We apply a set of requirements on the RTPC tracks to select the good ones:

- Hits from more than 4 pads
- Positive **curvature**
- How far the 1st ionization (**sdist**)
- How far the **last** ionization (**edist**)
- Helix fit quality (χ^2)
- Vertex correspondence (Δz)



The two modules of the RTPC have different levels of performance



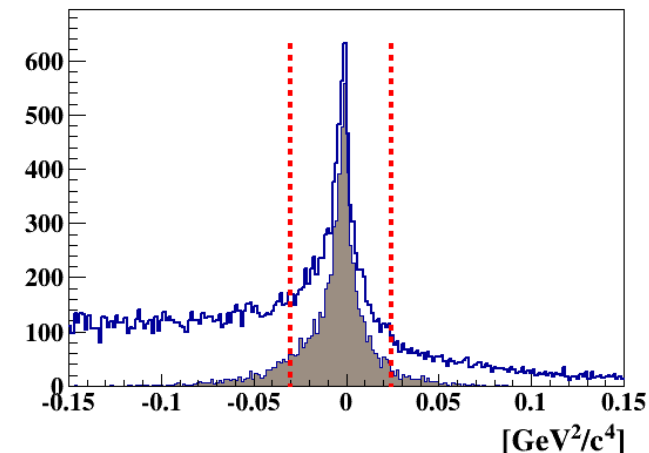
DVCS events selection (1/2)

We select **COHERENT** events which have:

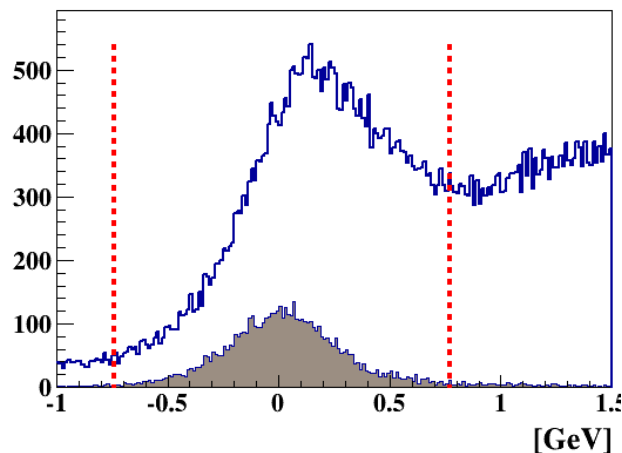
- ◇ Only one good electron, at least one photon and only one good ^4He .
- ◇ $E_\gamma > 2 \text{ GeV}$, $W > 2 \text{ GeV}/c^2$, $(E_b - E_{e'})/E_b < 0.85$ and $Q^2 > 1 \text{ GeV}^2$.
- ◇ Exclusivity cuts (3 sigmas).

- In **BLUE**, **coherent** events before all exclusivity cuts.
- In shaded **BROWN**, **coherent** DVCS events which pass all the other exclusivity cuts **except** the ONE ON the quantity itself.

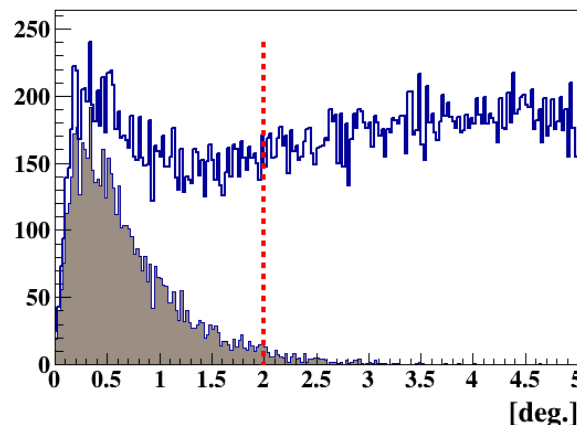
$e^4\text{He}\gamma\text{X}$: Missing M^2



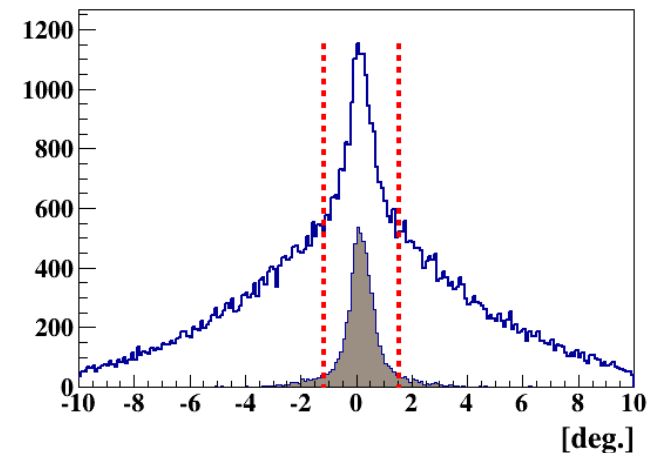
$e^4\text{He}\gamma\text{X}$: Missing E



$\theta(\gamma, e^4\text{HeX})$



$(\gamma, \gamma^*) : (\gamma^*, ^4\text{He}) :: \Delta\phi$



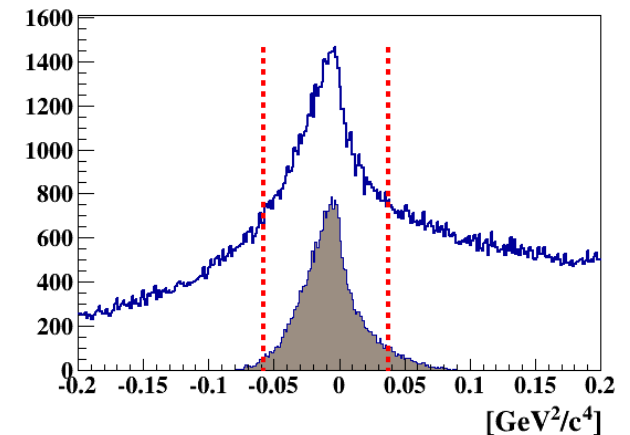
DVCS events selection (2/2)

We select **INCOHERENT** events which have:

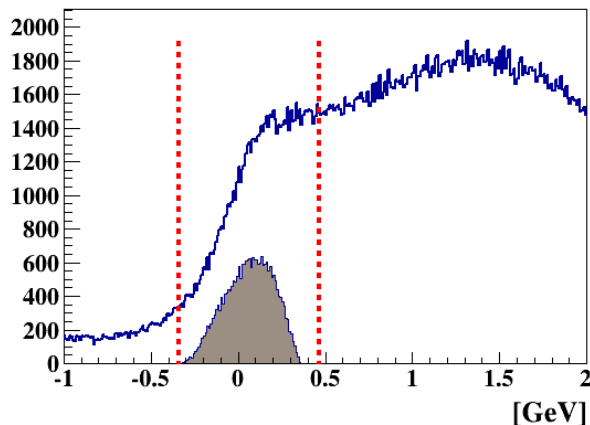
- ◇ Only one good electron, at least one photon and only one good p.
- ◇ $E_\gamma > 2 \text{ GeV}$, $W > 2 \text{ GeV}/c^2$, $(E_b - E_{e'})/E_b < 0.85$ and $Q^2 > 1 \text{ GeV}^2$.
- ◇ Exclusivity cuts (3 sigmas).

- In **BLUE**, **incoherent** events before all exclusivity cuts.
- In shaded **BROWN**, **incoherent** DVCS events which pass all the other exclusivity cuts **except** the ONE ON the quantity itself.

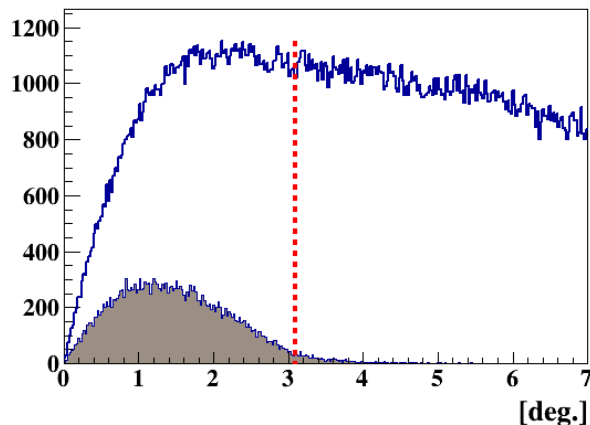
ep γ : Missing M^2



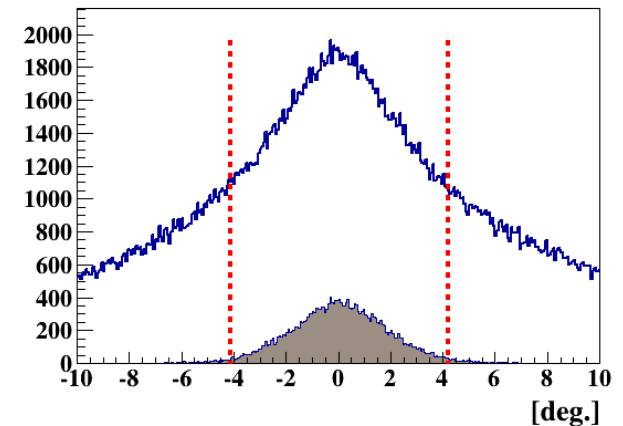
ep γ : Missing E



$\theta(\gamma, \text{epX})$



$(\gamma, \gamma^*):(\gamma^*, p) :: \Delta \phi$



Monte Carlo simulation (1/2)

◇ We use Monte Carlo for two goals:

- Understanding the behavior of each particle type within our detectors
- Calculate the acceptance ratio for the purpose of the DVCS background subtraction

◇ Simulation stages:

- **Event generator:** Events are generated in the measured phase-space (Q^2 , x_B , $-t$, ϕ_h) following this parametrization of the cross section:

$$\frac{d^4\sigma}{dQ^2 dx_B dt d\phi_h} \propto \left(\frac{Q_0^2}{Q^2}\right)^\alpha * \frac{1}{1 + \left(\frac{x_B - x_c}{c}\right)^2} * \frac{1}{(1 + bt)^\beta} * (1 - d(1 - \cos(\phi_h))).$$

Evolution in Q^2 ,
 $Q_0^2 = 1 \text{ GeV}^2$

Reproduces the PDFs
shape in the valence
region

Corresponds to
parametrization of
the $^4\text{He}(p)$ FFs

The dependence on A_h
(DVCS, BH, π^0)

- **Simulation (GSIM):** GEANT3, describes the detectors' response to the different particles.
- **Smearing (GPP):** Makes the simulation more realistic by smearing the positions, energy and time.
- **Reconstruction (RECSIS):** (ADCs, TDCs) \rightarrow physical quantities.

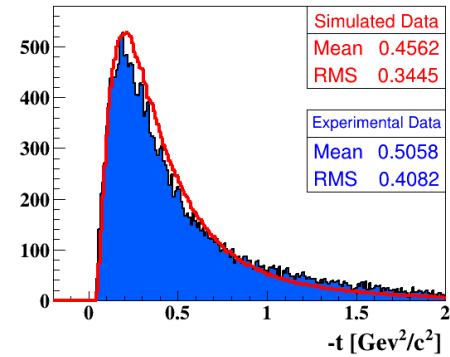
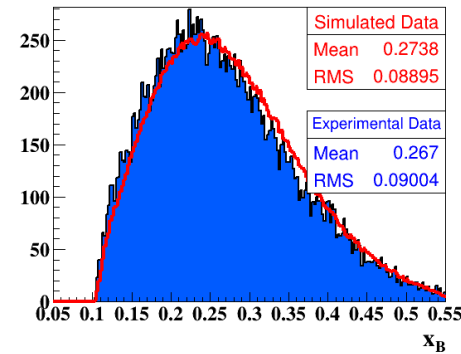
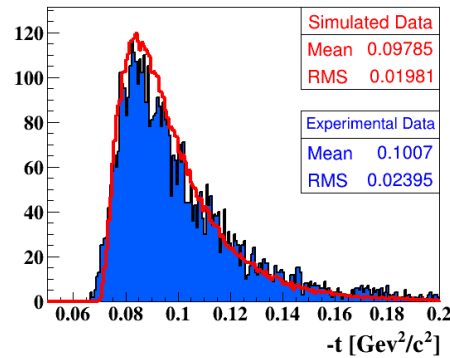
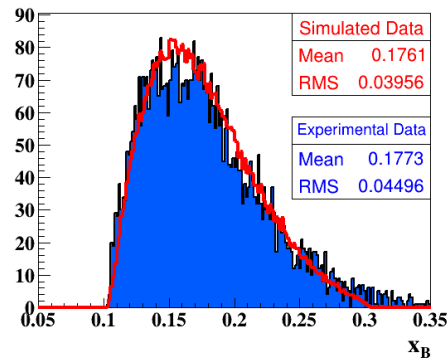
Monte Carlo simulation: Comparison with data (2/2)

- Apply the same DVCS criteria on the simulated data with an equivalent exclusive cuts.

Coherent DVCS

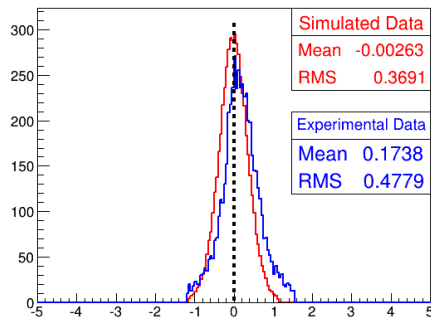
Incoherent DVCS

* In terms of the kinematics

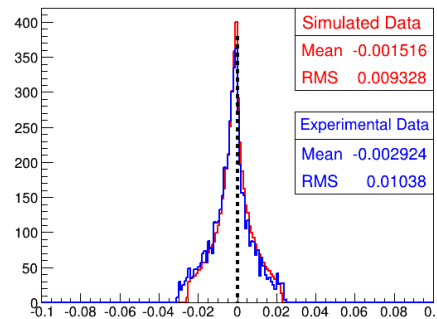


* In terms of the exclusivity variables

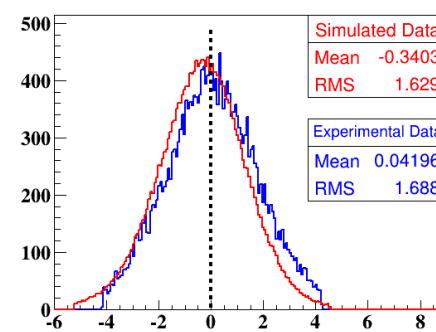
$(\gamma, \gamma^*) : (\gamma^*, {}^4\text{He}) :: \Delta \phi$ [Deg.]



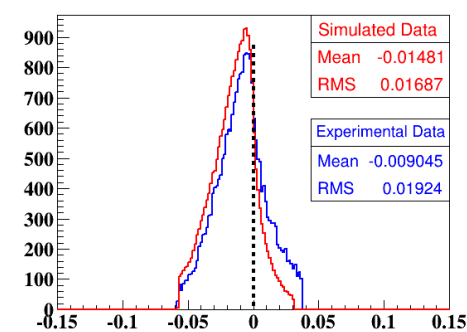
$e^4\text{He}\gamma$: Missing M^2 [GeV²/c⁴]



$(\gamma, \gamma^*) : (\gamma^*, p) :: \Delta \phi$ [Deg.]



$e'\gamma$: Missing M^2 [GeV/c²]



Adequate agreement between data and simulation

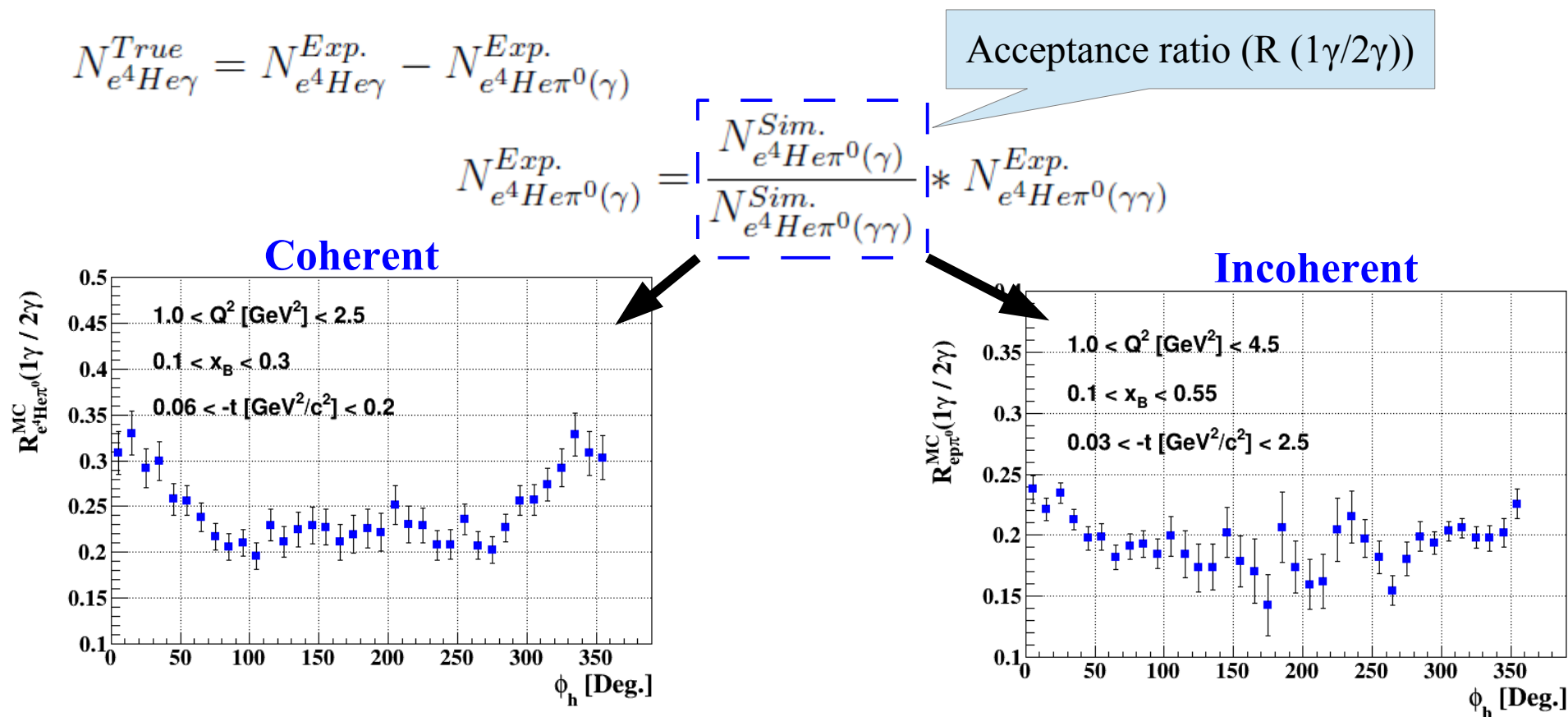
Background subtraction

◇ With our kinematics, the main background comes from the exclusive π^0 channel,

$$e^4He \rightarrow e^4He\pi^0 \rightarrow e^4He\gamma\gamma \quad ep \rightarrow ep\pi^0 \rightarrow ep\gamma\gamma$$

in which **one photon** from π^0 decay is detected and passes the DVCS selection.

◇ We combine real data with simulation to compute the contamination of π^0 to DVCS.



◇ Background yield ratio \sim **2-4%** (**8-11%**) in $e^-^4He\gamma$ ($e^-p\gamma$) DVCS channel.

Coherent beam-spin asymmetries

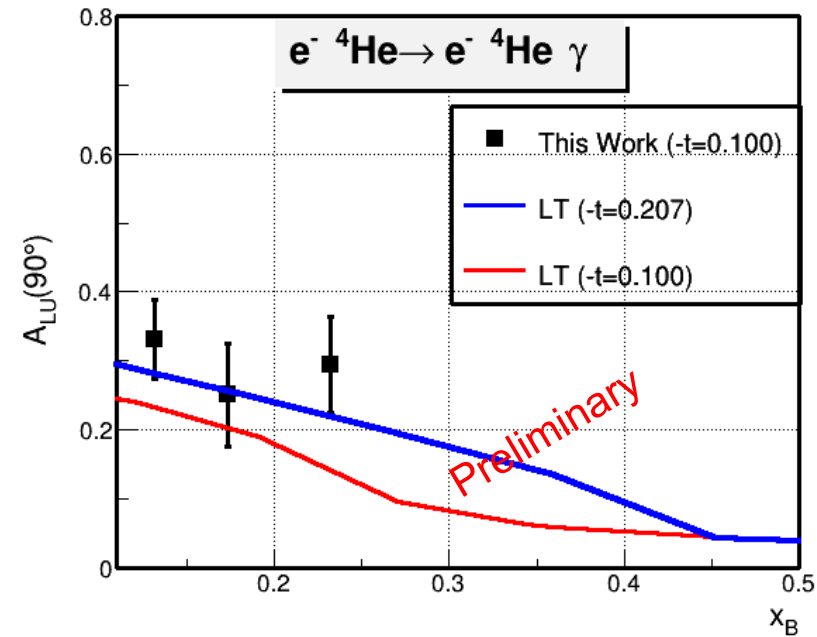
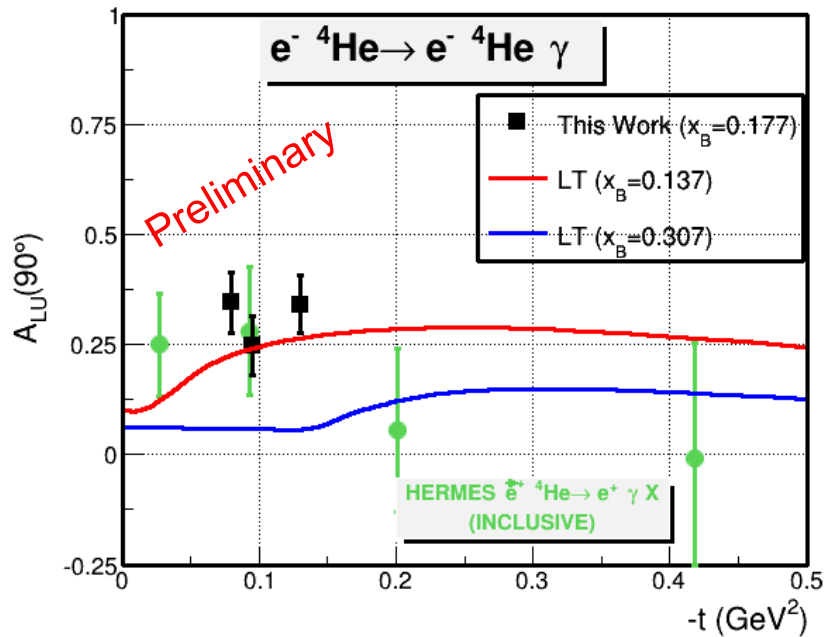
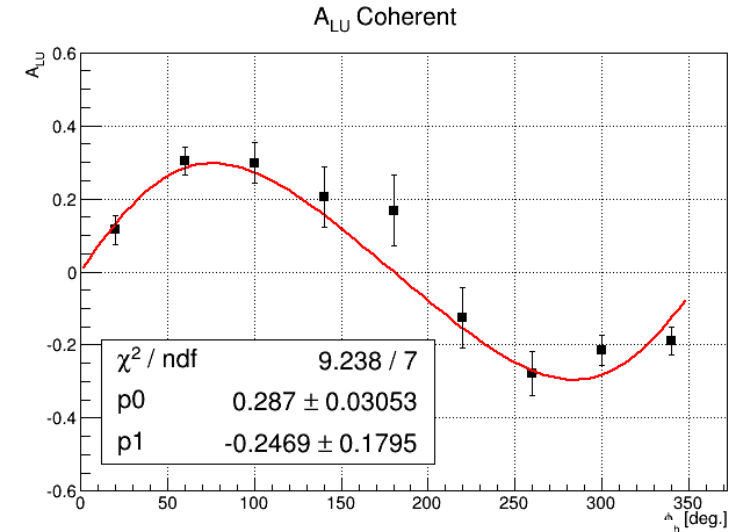
→ Probed coherent kinematical regions:

$$0.06 < -t < 0.2 \rightarrow \langle -t \rangle = 0.10 [\text{GeV}^2]$$

$$1.0 < Q^2 < 2.5 \rightarrow \langle Q^2 \rangle = 1.49 [\text{GeV}^2]$$

$$0.1 < x_B < 0.3 \rightarrow \langle x_B \rangle = 0.18$$

- Due to **statistical constraints**, we constructed **2D** bins $-t$ or x_B or Q^2 versus ϕ
- Fit A_{LU} : $p_0 * \sin(\phi) / (1 + p_1 * \cos(\phi))$



[1] LT: S. Liuti and S. K. Taneja. Phys. Rev., C72:032201, 2005.

[2] A. Airapetian, et al., Phys Rev. C 81, 035202 (2010).

Helium-4 Compton form factor

$$A_{LU}(\phi) = \frac{\alpha_0(\phi) * Im(\mathcal{H}_A)}{\alpha_1(\phi) + \alpha_2(\phi)Re(\mathcal{H}_A) + \alpha_3(\phi)(Im(\mathcal{H}_A)^2 + Re(\mathcal{H}_A)^2)}$$

$$\alpha_0 \sim 10^{-2}, \alpha_1 \sim 1, \alpha_2 \sim 10^{-2}, \boxed{\alpha_3 \sim 10^{-4}} \quad \text{Suppressed by 2 orders of magnitude}$$

$$\alpha_0(\phi) = a \sin(\phi)$$

$$\alpha_1(\phi) = b + c \cos(\phi) + \boxed{d \cos(2\phi)}$$

$$\alpha_2(\phi) = h + f \cos(\phi)$$

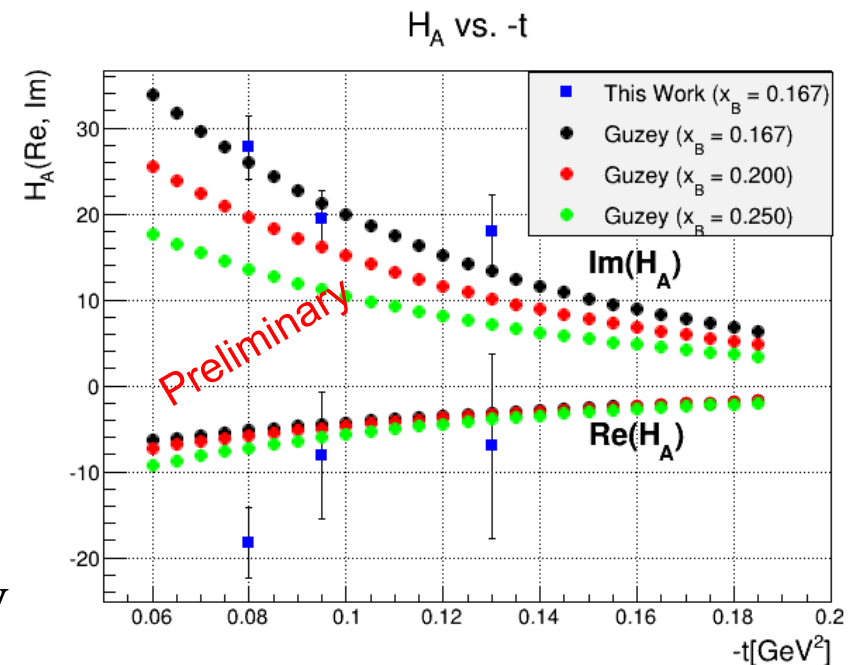
Expected to be small magnitude

- Using the kinematical calculable factors (a, b, c, h and f) and the fitted coherent ALU @ 90° vs. $\langle -t \rangle$

$$p_0 * \sin(\phi) / (1 + p_1 * \cos(\phi))$$

→ Extracted the real and the imaginary parts of the Compton form factor.

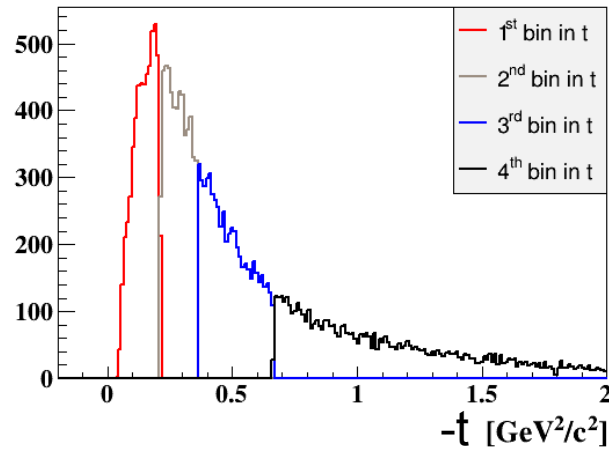
- We have “significant” trends with t and xB as well.



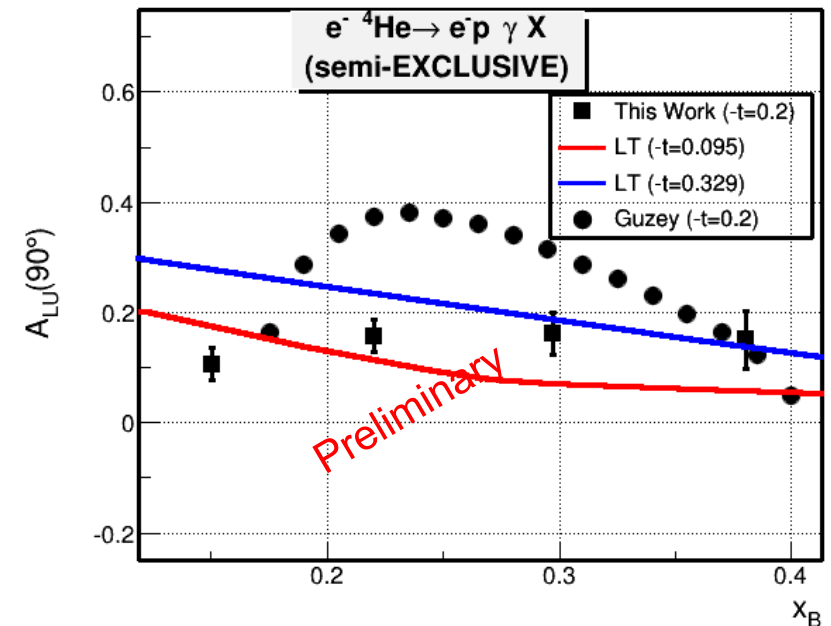
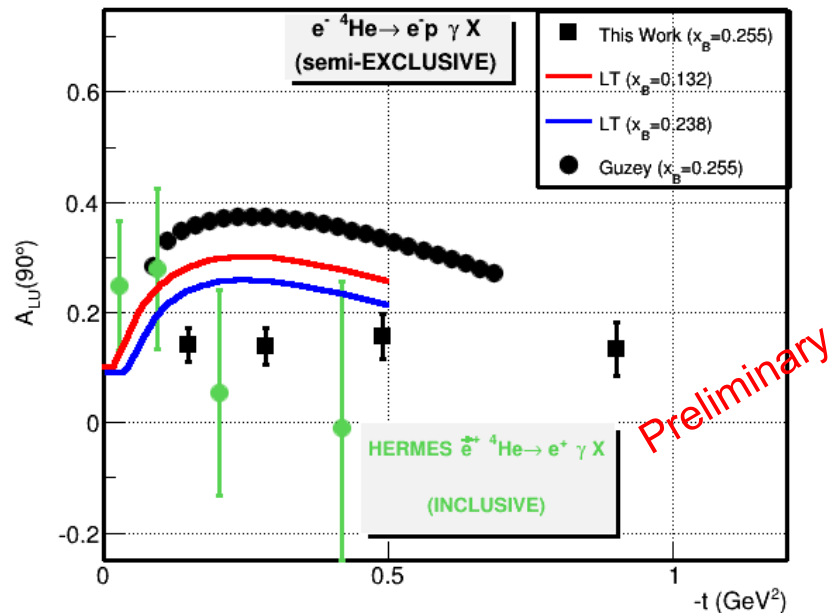
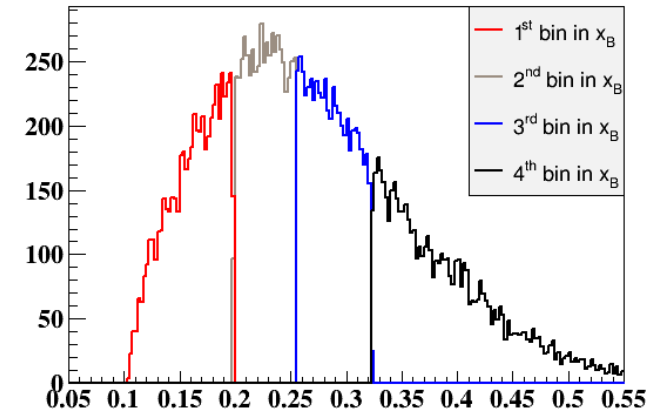
Incoherent beam-spin asymmetries

◇ Probed kinematical regions: $1.0 < Q^2 < 4.5$ [GeV²] $\rightarrow \langle Q^2 \rangle = 2.20$ [GeV²]

-t of epy events



x_B of epy events

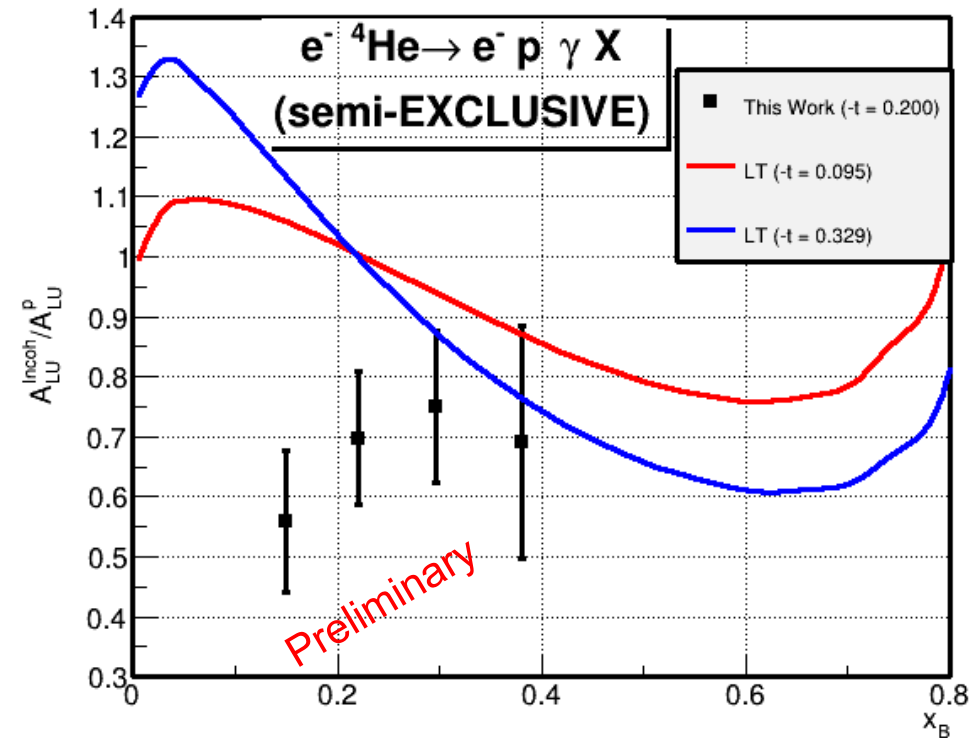
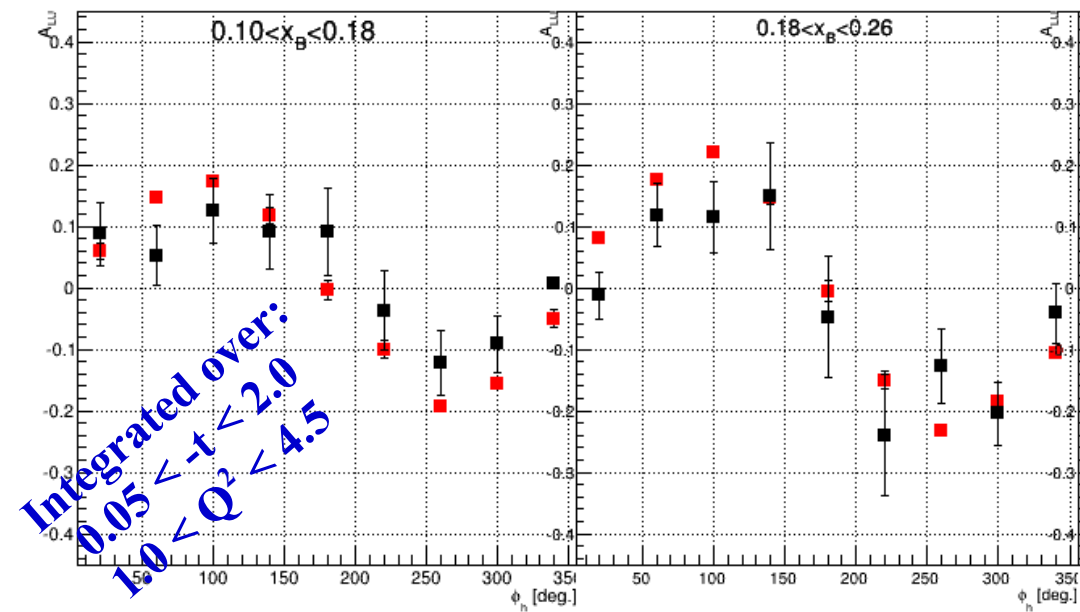


- [1] LT: S. Liuti and S. K. Taneja, Phys. Rev., C72:032201, 2005.
 [2] A. Airapetian, et al., Phys Rev. C 81, 035202 (2010).

EMC ratio (1/3)

◇ We compared our measured incoherent asymmetries (Black points) with the asymmetries measured in CLAS DVCS experiment on the proton (Red Points).

A_{LU} vs. ϕ in x_B bins



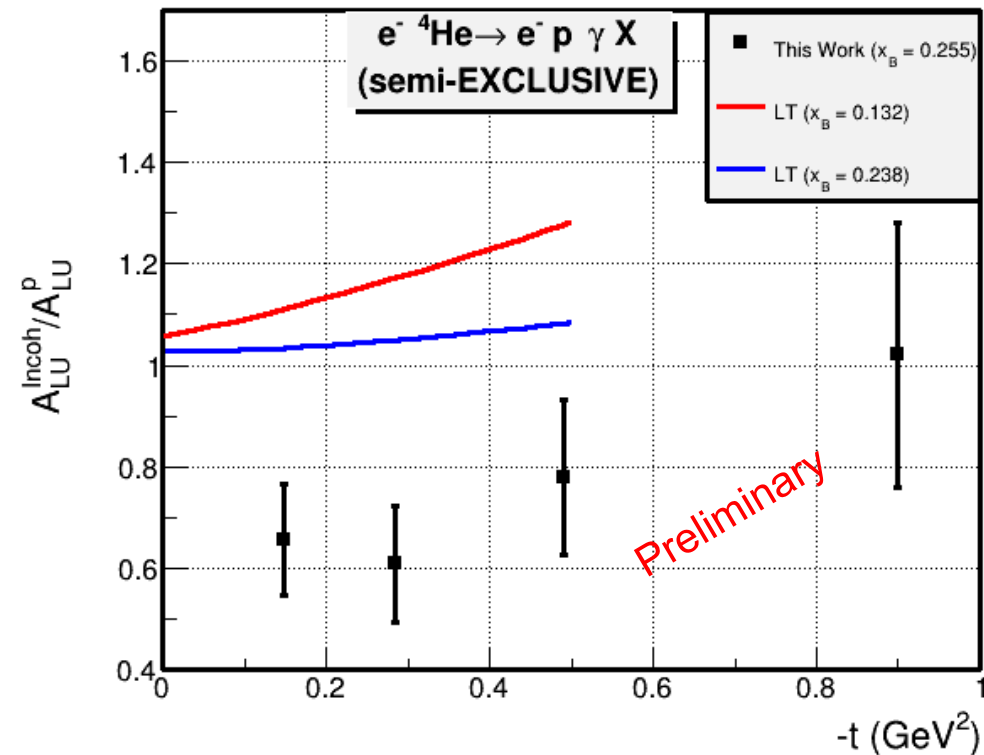
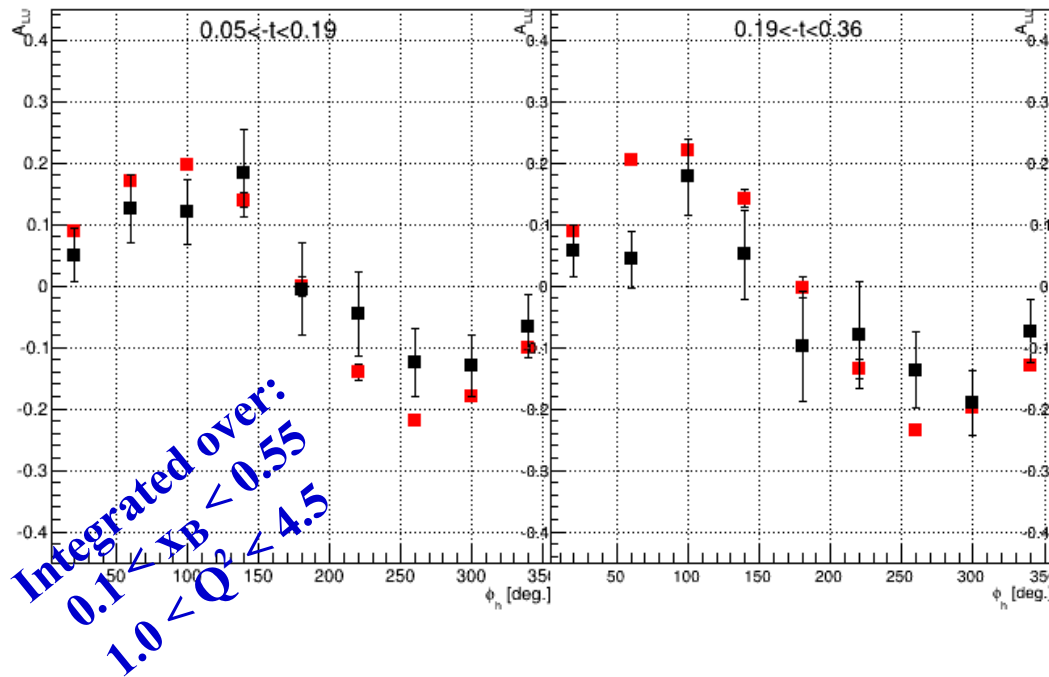
◇ The bound proton shows a lower asymmetry relative the free one in the different bins in x_B .

EMC ratio (2/3)

◇ Black points: Our measured incoherent asymmetries

Red Points: The asymmetries measured in CLAS DVCS experiment on the proton (e1-dvcs)

A_{LU} vs. ϕ in $-t$ bins



◇ At small $-t$, the bound proton shows lower asymmetry than the free one.

◇ At high $-t$, the two asymmetries are compatible.

EMC ratio (3/3)

◇ Comparing the coherent asymmetry to the free proton's asymmetry:

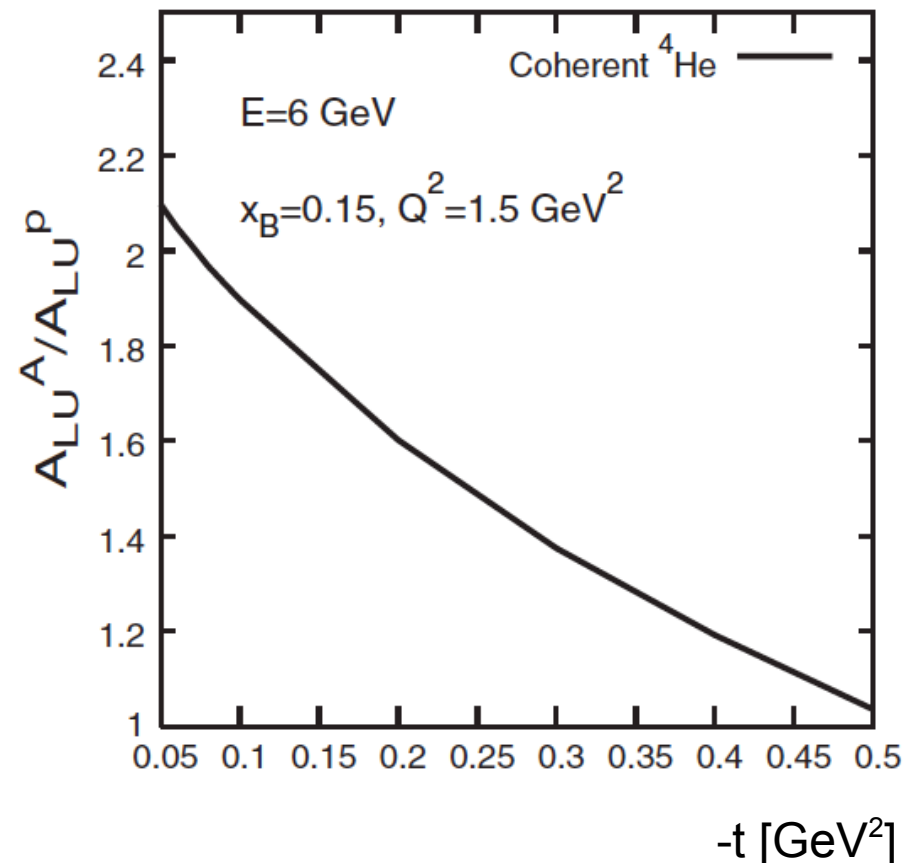
$$\langle -t \rangle = 0.13 \text{ [GeV}^2\text{]}$$

$$\langle Q^2 \rangle = 1.49 \text{ [GeV}^2\text{]}$$

$$\langle x_B \rangle = 0.16$$

$$\langle A_{\text{LU}}^{4\text{He}} / A_{\text{LU}}^{\text{p}} \rangle = 0.34 / 0.21 = 1.6$$

Consistent with the enhancement suggested by the Impulse Approximation Model of Vadim Guzey



[V. Guzey, PRC 78(2008) 025211]

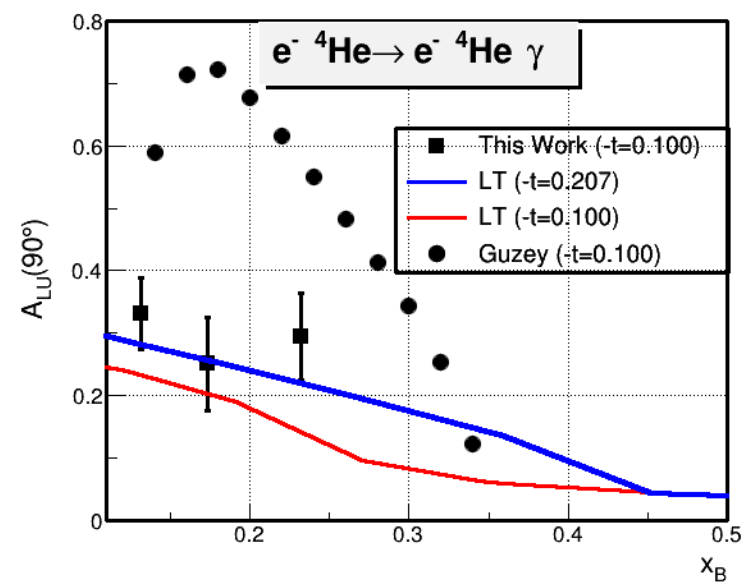
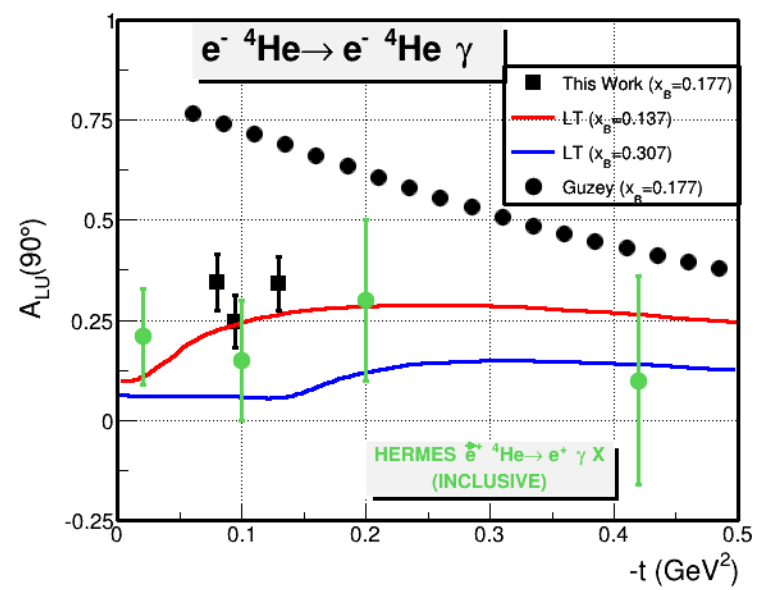
Conclusions

- ◇ The exclusive DVCS off ^4He was measured for the first time with our experiment
- ◇ Preliminary asymmetries were extracted and compared with theoretical predictions
- ◇ With our available statistics, the bound proton has shown a different trend compared to the free one
- ◇ Perspectives:
 - Final results soon
 - Proposing a new ^4He DVCS experiment with JLab upgrade.

Thanks for your attention

Backup slides







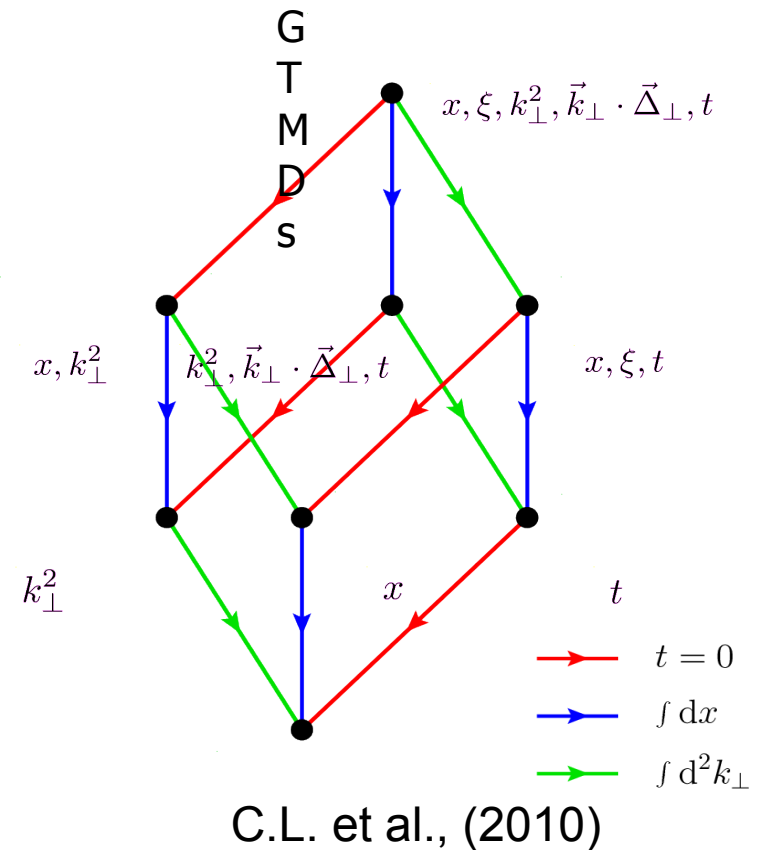
Hadronic structure functions (3/3)

Structure functions that quantify the properties of the partons in a hadron:

- Form Factors (FFs)
- Parton Distribution Functions (PDFs)
- Transverse Momentum Distributions (TMDs)
- Generalized Parton Distributions (GPDs)
- Generalized Transverse Momentum Distributions (GTMDs)

- Most general functions that describe the proton structure in **5** dimensions.
- Connected to the so-called Wigner distributions via 2D Fourier transform over Δ .

[See A. V. Belitsky, X. Ji, F. Yuan; Phys. Rev. D 69 (2004) 074014.]

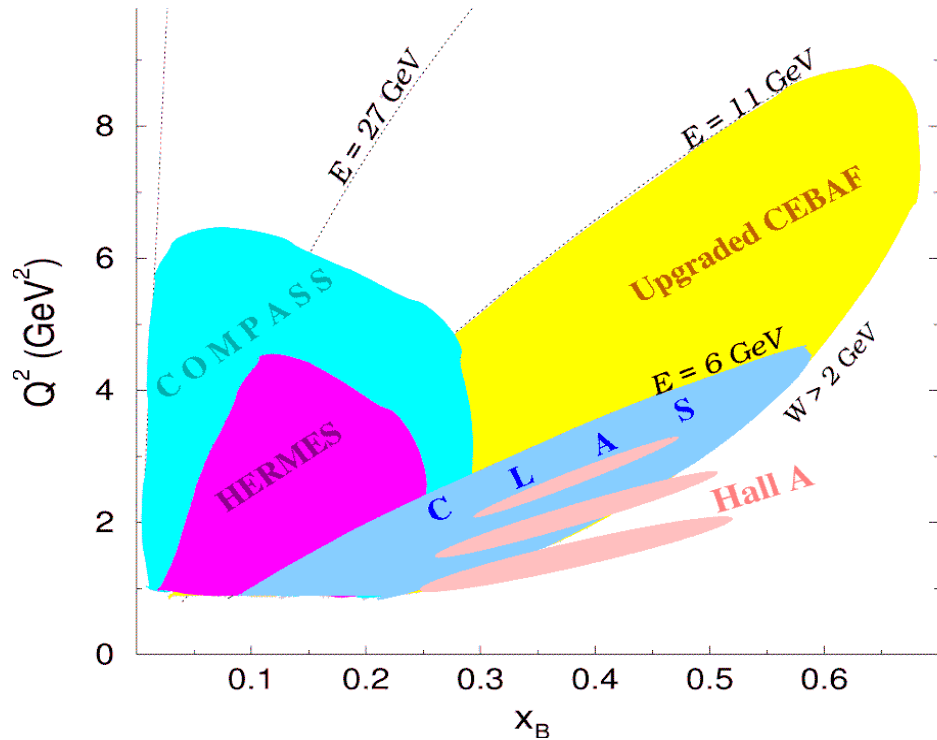


x : Parton's longitudinal momentum

k_{\perp} : Parton's transverse momentum

Δ : Momentum transfer to the nucleon

DVCS experiments worldwide

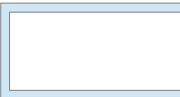


JLAB	
<i>Hall A</i>	<i>Hall B</i>
p,n-DVCS: (pol.) X-sec	p-DVCS: BSA,LTSA, DSA, X-sec Helium-4: BSA

CERN
COMPASS
p-DVCS: X-sec,BSA,BCA, tTSA,lTSA,DSA

DESY	
<i>HERMES</i>	<i>H1/ZEUS</i>
p-DVCS BSA,BCA, TTSA, LTSA,DSA	p-DVCS X-sec,BCA

Promising future experiments with JLab upgrade and COMPASSII



Nucleon DVCS spin observables

$$Re\mathcal{H}(\xi, t) = \mathcal{P} \int_{-1}^1 dx [H(x, \xi, t) - H(-x, \xi, t)] [C^+(x, \xi)]$$

Quark propagator

$$Im\mathcal{H}(\xi, t) = H(\xi, \xi, t) - H(-\xi, \xi, t)$$

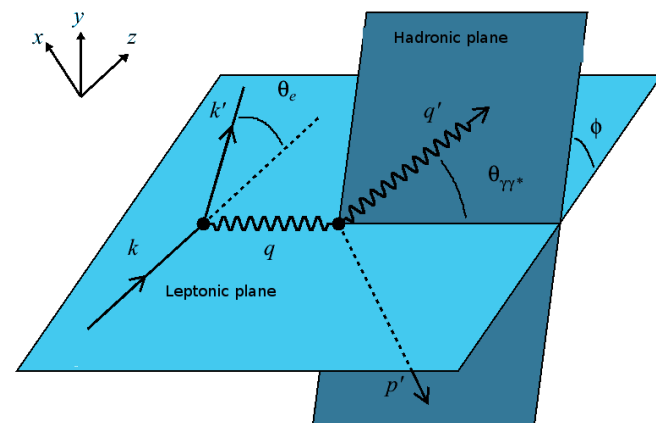
$$C^+(x, \xi) = \frac{1}{x - \xi} + \frac{1}{x + \xi}$$

$$\mathcal{H}(\xi, t) = Re\mathcal{H}(\xi, t) - i\pi Im\mathcal{H}(\xi, t)$$

$$\sigma(x_B, Q^2, t, \phi_h) \sim |\mathcal{T}_{DVCS} + \mathcal{T}_{BH}|^2$$

$$\Delta\sigma(x_B, Q^2, t, \phi_h) = \sigma^+ - \sigma^-$$

$$A(x_B, Q^2, t, \phi_h) = \frac{\sigma^+ - \sigma^-}{\sigma^+ + \sigma^-}$$



- **L** polarized beam, **U**npolarized target
- **U**npolarized beam, **L** polarized target
- **U**npolarized beam, **T** polarized target
- **L** polarized beam, **L** polarized target

Observable	proton	neutron
$\Delta\sigma_{LU}$	$Im \left\{ \mathcal{H}_p, \tilde{\mathcal{H}}_p, \mathcal{E}_p \right\}$	$Im \left\{ \mathcal{H}_n, \tilde{\mathcal{H}}_n, \mathcal{E}_n \right\}$
$\Delta\sigma_{UL}$	$Im \left\{ \mathcal{H}_p, \tilde{\mathcal{H}}_p \right\}$	$Im \left\{ \mathcal{H}_n, \mathcal{E}_n, \tilde{\mathcal{E}}_n \right\}$
$\Delta\sigma_{UT}$	$Im \left\{ \mathcal{H}_p, \mathcal{E}_p \right\}$	$Im \left\{ \mathcal{H}_n \right\}$
$\Delta\sigma_{LL}$	$Re \left\{ \mathcal{H}_p, \tilde{\mathcal{H}}_p \right\}$	$Re \left\{ \mathcal{H}_n, \mathcal{E}_n, \tilde{\mathcal{E}}_n \right\}$

$\alpha_i(\phi)$ coefficients appearing in the BSA expression

$$\begin{aligned}
 \alpha_0(\phi) &= 8 K x_A (1 + \epsilon^2)^2 (2 - y) F_A \sin(\phi) \\
 \alpha_1(\phi) &= c_0^{BH} + c_1^{BH} \cos(\phi) + c_2^{BH} \cos(2\phi) \\
 \alpha_2(\phi) &= 8 \frac{x_A}{y} (1 + \epsilon^2)^2 F_A \left[K(2y - y^2 - 2) \cos(\phi) \right. \\
 &\quad \left. - (2 - y) \left(\frac{t}{Q^2} \right) \left((2 - x_A)(1 - y) - (1 - x_A)(2 - y)^2 \left(1 - \frac{t_{min}}{Q^2} \right) \right) \right] \\
 \alpha_3(\phi) &= 2 \frac{x_A^2 t}{Q^2} (2 - 2y + y^2) (1 + \epsilon^2)^2 \mathcal{P}_1(\phi) \mathcal{P}_2(\phi)
 \end{aligned}$$

◇ The Fourier coefficients of the BH amplitude for a spin-0 target can be expressed as:

$$\begin{aligned}
 c_0^{BH} &= \left[\left\{ (2 - y)^2 + y^2 (1 + \epsilon^2)^2 \right\} \left\{ \frac{\epsilon^2 Q^2}{t} + 4(1 - x_A) + (4x_A + \epsilon^2) \frac{t}{Q^2} \right\} \right. \\
 &\quad \left. + 2\epsilon^2 \left\{ 4(1 - y)(3 + 2\epsilon^2) + y^2(2 - \epsilon^4) \right\} - 4x_A^2 (2 - y)^2 (2 + \epsilon^2) \frac{t}{Q^2} \right. \\
 &\quad \left. + 8K^2 \frac{\epsilon^2 Q^2}{t} \right] F_A^2, \\
 c_1^{BH} &= -8(2 - y)K \left\{ 2x_A + \epsilon^2 - \frac{\epsilon^2 Q^2}{t} \right\} F_A^2, \\
 c_2^{BH} &= 8K^2 \frac{\epsilon^2 Q^2}{t} F_A^2,
 \end{aligned}$$



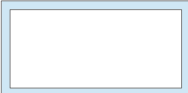
The correlation matrix between coherent fit parameters

-t bin:

EXT PARAMETER					FIRST
NO.	NAME	VALUE	ERROR	STEP SIZE	DERIVATIVE
1	p0	3.44813e-01	5.62771e-02	6.48807e-05	-4.44260e-04
2	p1	-3.50787e-02	3.29259e-01	3.79811e-04	5.27253e-05
1	p0	2.46885e-01	5.76178e-02	3.98343e-05	5.35585e-04
2	p1	-4.63055e-01	2.50428e-01	1.73172e-04	-6.46587e-05
1	p0	3.41273e-01	5.44831e-02	7.49783e-05	-9.17018e-04
2	p1	-1.65254e-02	2.87350e-01	3.95405e-04	1.63433e-04

x_B bins:

EXT PARAMETER					FIRST
NO.	NAME	VALUE	ERROR	STEP SIZE	DERIVATIVE
1	p0	3.31482e-01	4.67747e-02	7.80803e-05	-5.92762e-03
2	p1	1.30716e-01	2.73364e-01	4.55543e-04	4.38945e-04
1	p0	2.51482e-01	6.59560e-02	3.80359e-05	-1.00104e-02
2	p1	-5.38260e-01	2.61527e-01	1.50322e-04	1.58311e-03
1	p0	2.95191e-01	6.66935e-02	5.95809e-05	4.84575e-04
2	p1	-2.47236e-01	2.96955e-01	2.65219e-04	-2.07350e-05



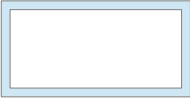
The correlation matrix between incoherent fit parameters

-t bin:

EXT PARAMETER			STEP		FIRST
NO.	NAME	VALUE	ERROR	SIZE	DERIVATIVE
1	p0	1.41307e-01	2.68771e-02	2.33962e-05	6.11524e-06
2	p1	-4.59316e-02	4.33266e-01	3.77153e-04	-4.67165e-08
1	p0	1.38396e-01	2.90665e-02	3.62930e-05	-5.69892e-03
2	p1	-5.99352e-02	3.98839e-01	4.96849e-04	5.21778e-04
1	p0	1.56694e-01	3.61020e-02	4.43406e-05	-8.89337e-03
2	p1	-2.56722e-01	3.86908e-01	4.76556e-04	7.28503e-04

x_B bins:

EXT PARAMETER			STEP		FIRST
NO.	NAME	VALUE	ERROR	SIZE	DERIVATIVE
1	p0	1.06571e-01	2.46824e-02	2.79274e-05	3.21506e-04
2	p1	1.67206e-01	4.32436e-01	4.89767e-04	6.19943e-04
1	p0	1.56996e-01	2.84421e-02	3.91407e-05	3.14828e-02
2	p1	4.01100e-01	4.35838e-01	6.05845e-04	-1.74217e-04
1	p0	1.62795e-01	3.24642e-02	4.72162e-05	-1.68329e-03
2	p1	6.73701e-02	3.34978e-01	4.87360e-04	1.54408e-04
1	p0	1.50467e-01	4.84699e-02	2.15941e-05	1.36698e-02
2	p1	-4.29531e-01	3.13659e-01	1.38203e-04	-4.00935e-03

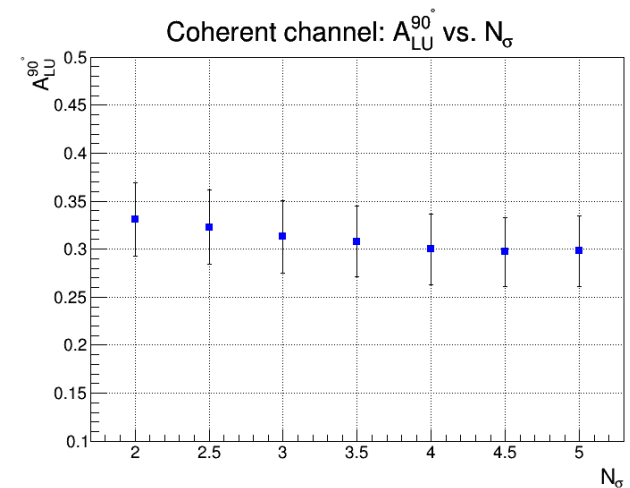
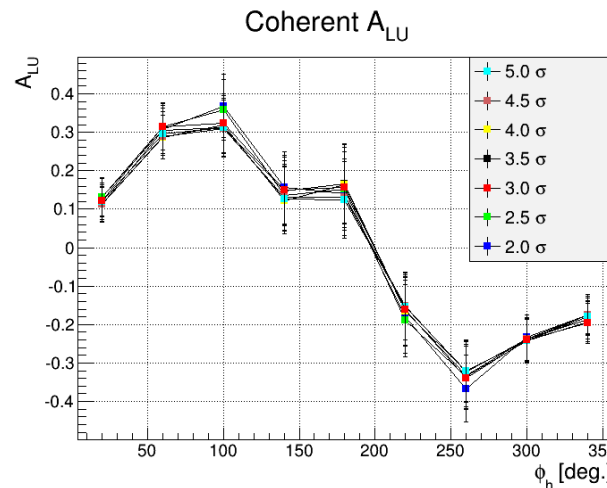
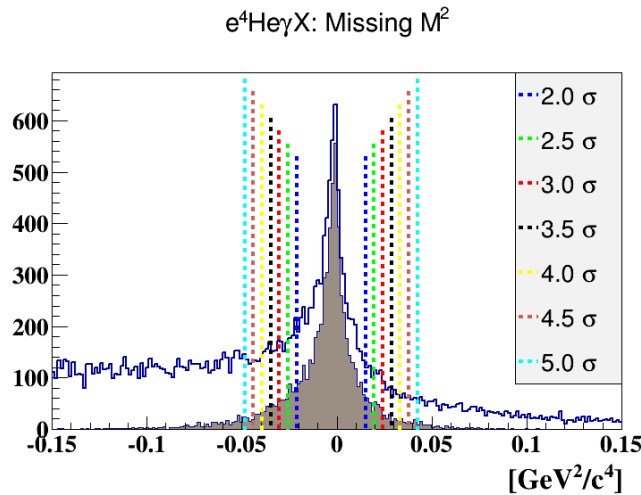


Beam-spin asymmetry uncertainties (1/2)

◇ **Statistical** uncertainty: $\Delta A_{LU}^{stat} = \frac{1}{P_B} \sqrt{\frac{1 - (P_B A_{LU})^2}{N^+ - N^-}}$

◇ **Systematic** uncertainties: Most of the experimental systematic uncertainties, such as efficiencies and normalizations, cancel in the asymmetry ratio. **Nevertheless**, some sources still induce some uncertainties:

→ **DVCS selection cuts**: Fix all the exclusivity cuts except one



⇒ ..he maximum variation in the coherent (incoherent) A_{LU} is **3.7%** (**4.0%**)

→ **Background subtraction**: - Use two generating models to calculate R(1γ/2γ)
- Repeat the analysis by ±20% on R(1γ/2γ)

⇒ Coherent (Incoherent) uncertainty is **0.6%** (**2.0%**)

Beam-spin asymmetry uncertainties (2/2)

- **Beam polarization:** The precision of the Hall-B Møller polarimeter is 3.5 % [1] which is induced as systematic uncertainty on the measured A_{LU} . $\left(\frac{\Delta A_{LU}^{sys.p}}{A_{LU}} = \frac{\Delta p}{p}\right)$
- **Radiative corrections:** Anderi Afanasev and his collaborators performed one-loop electromagnetic corrections on the outgoing DVCS electron [2]. As a result, they found that the induced A_{LU} does not exceed 0.1% at 4.25 GeV electron beam energy and $Q^2=1.25 \text{ GeV}^2$.

□ Total relative systematic uncertainties:

Systematic source	Coherent channel	Incoherent channel
DVCS cuts	4 %	3.7 %
Beam polarization	3.5%	3.5%
π^0 subtraction	0.6%	2.0%
Radiative corrections	0.1%	0.1%
Total	5.3%	5.5%

These experimental uncertainties are involved
in our **asymmetries** and will propagate into the extracted **CFFs**

[1] J. M. Grames et al., Phys. Rev. Spec. TOPICS - Accelerators and Beams, Vol.7 , 042802, 2004.

[2] A.V. Afanasev, M.I. Konchatnij, and N.P. Merenkov, . arXiv:hep-ph/050709v1, 2005.